

# Lipid nanoparticle mRNA systems containing high levels of sphingomyelin engender higher protein expression in hepatic and extra-hepatic tissues

Nisha Chander,<sup>1</sup> Genc Basha,<sup>1</sup> Miffy Hok Yan Cheng,<sup>1</sup> Dominik Witzigmann,<sup>2</sup> and Pieter R. Cullis<sup>1,2</sup>

<sup>1</sup>Department of Biochemistry and Molecular Biology, University of British Columbia, 2350 Health Sciences Mall, Vancouver, BC V6T 1Z3, Canada; <sup>2</sup>NanoVation Therapeutics, 2405 Wesbrook Mall, Vancouver, BC V6T 1Z3, Canada

**Lipid nanoparticles (LNPs) for delivery of mRNA usually contain ionizable lipid/helper lipid/cholesterol/PEG-lipid in molar ratios of 50:10:38.5:1.5, respectively. These LNPs are rapidly cleared from the circulation following intravenous (i.v.) administration, limiting uptake into other tissues. Here, we investigate the properties of LNP mRNA systems prepared with high levels of “helper” lipids such as 1,2-distearoyl-sn-glycero-3-phosphorylcholine (DSPC) or N-(hexadecanoyl)-sphing-4-enine-1-phosphocholine (egg sphingomyelin [ESM]). We show that LNP mRNAs containing 40 mol % DSPC or ESM have a unique morphology with a small interior “solid” core situated in an aqueous compartment that is bounded by a lipid bilayer. The encapsulated mRNA exhibits enhanced stability in the presence of serum. LNP mRNA systems containing 40 mol % DSPC or ESM exhibit significantly improved transfection properties *in vitro* compared with systems containing 10 mol % DSPC or ESM. When injected i.v., LNP mRNAs containing 40 mol % ESM exhibit extended circulation lifetimes compared with LNP mRNA systems containing 10 mol % DSPC, resulting in improved accumulation in extrahepatic tissues. Systems containing 40 mol % ESM result in significantly improved gene expression in spleen and bone marrow as well as liver post i.v. injection compared with 10 mol % DSPC LNP mRNAs. We conclude that LNP mRNAs containing high levels of helper lipid provide a new approach for transfecting hepatic and extrahepatic tissues.**

## INTRODUCTION

Lipid nanoparticles (LNPs) are clinically validated systems for delivery of messenger RNA (mRNA) *in vivo* having been used in COVID-19 mRNA vaccines to express viral genes in muscle and antigen-presenting cells following intramuscular administration.<sup>1</sup> There is considerable additional literature detailing the ability of LNP mRNA systems to transfect the liver (hepatocytes) following intravenous (i.v.) administration, leading to many more potential therapeutic applications.<sup>1–4</sup> Liver-tropic LNP mRNA therapeutics are currently being developed to treat cancer, atherosclerosis, heart failure, and rare diseases using gene editing or protein replacement approaches.<sup>2,3,5</sup> All these formulations use LNP lipid compositions consisting of ionizable lipid/helper lipid/cholesterol/PEG-lipid in the approximate molar ratios 50:10:38.5:1.5, respectively. The helper lipid

commonly used is 1,2-distearoyl-sn-glycero-3-phosphorylcholine (DSPC). Here, we refer to this lipid composition as the “Onpattro” formulation as similar lipid ratios are used in Onpattro, the clinically approved siRNA-based nanomedicine used to treat transthyretin-induced amyloidosis.<sup>6</sup>

Efforts to transfect extrahepatic tissues via i.v. administration have been less successful. Approximately 90% of the injected dose of LNP mRNA formulations with the Onpattro lipid composition is cleared to the liver within 30 min of i.v. administration,<sup>7</sup> limiting access to other tissues. Extended circulation lifetimes necessary to access non-liver tissues can be achieved by incorporating PEG-lipids that remain associated with the LNP following i.v. administration.<sup>8,9</sup> However, the presence of a PEG coating inhibits cell uptake and delivery of mRNA contents.<sup>9,10</sup> Incorporation of positively charged lipids can enhance transfection in a number of extrahepatic tissues following i.v. administration.<sup>11</sup> Unfortunately, such lipids can be toxic, potentially limiting clinical applications.<sup>12,13</sup>

In recent work we have shown for the ethanol dilution/rapid mixing formulation technique that incorporation of increasing amounts of triolein (TO), a non-polar lipid that is not soluble in lipid bilayers, in mixtures with DSPC/Chol at molar ratios of 40:40:20 (DSPC/Chol/TO, respectively) results in LNPs that exhibit an interior solid core structure surrounded by a lipid bilayer as visualized by cryogenic-transmission electron microscopy (cryo-TEM).<sup>14</sup> Similar structures are observed for LNP systems containing 40 mol % DSPC and reduced levels of ionizable cationic lipids, with or without an siRNA payload.<sup>15</sup> The structure of these systems is consistent with a lipid bilayer consisting of DSPC/Chol and an interior solid core consisting of the hydrophobic TO or oil form of the ionizable lipid surrounded by a lipid monolayer. Such systems offer interesting possibilities for long circulation properties given the long

Received 21 December 2022; accepted 8 June 2023;  
<https://doi.org/10.1016/j.omtm.2023.06.005>.

**Correspondence:** Pieter R. Cullis, Department of Biochemistry and Molecular Biology, University of British Columbia, 2350 Health Sciences Mall, Vancouver, BC V6T 1Z3, Canada.

**E-mail:** [pieterc@mail.ubc.ca](mailto:pieterc@mail.ubc.ca)



circulation lifetimes of DSPC/Chol liposomal systems used in cancer applications.<sup>16,17</sup>

Here, we examine the transfection properties of LNP mRNA systems containing high (up to 40 mol %) levels of DSPC or an alternative helper lipid, N-(hexadecanoyl)-sphing-4-enine-1-phosphocholine (egg sphingomyelin [ESM]), together with reduced levels (as low as 33 mol %) of the ionizable cationic lipid DLinMC3DMA (MC3) both *in vitro* and *in vivo*. For systems containing 40 mol % helper lipid we show that such systems can achieve mRNA trapping efficiencies greater than 90% and that they exhibit cryo-TEM morphology consisting of a “solid core” and an aqueous compartment that is partially or completely surrounded by a lipid bilayer. These systems exhibit transfection potencies *in vitro* that are comparable with or superior than Onpattro-based LNP mRNA systems that contain 10 mol % DSPC. Furthermore, we demonstrate that LNP mRNA systems containing 40 mol % ESM result in improved transfection potency in the liver, spleen, and bone marrow following systemic administration relative to LNPs with the Onpattro lipid composition. It is concluded that LNP mRNA systems containing high concentrations of helper lipids such as ESM represent a new class of mRNA delivery systems that can be used to transfect hepatic as well as extrahepatic tissues *in vivo*.

## RESULTS

### LNP mRNA systems containing 40 mol % ESM exhibit a solid core within a bilayer morphology as detected by cryo-TEM

As noted, the structure of LNP siRNA systems containing high levels of helper lipids such as DSPC can exhibit unusual morphology consisting of an inner solid core separated from an external bilayer by an aqueous compartment. To determine whether similar structures are observed for LNP mRNA systems formulated at high helper lipid contents we examined the morphology of LNP luc mRNA systems as the proportion of ESM helper lipid was increased.

LNP luc mRNA formulations were prepared using MC3 as the ionizable lipid and ESM as the helper lipid. The proportion of ESM was increased from 10 to 55 mol % at the expense of both ionizable lipid and cholesterol (keeping the MC3/Chol ratio constant). As shown in Table S1, mRNA encapsulation efficiencies >95% were achieved for LNPs containing 10–40 mol % ESM, whereas reduced entrapment efficiencies were observed at higher ESM levels. LNPs containing up to 50 mol % ESM exhibited diameters of ~50 nm and low polydispersity indices (PDIs), LNP mRNA systems containing 55 mol % ESM were larger (68 nm) and more polydisperse.

It would be expected that the morphology of the LNP mRNA systems containing increasingly high levels of ESM would exhibit progressively more bilayer structure as ESM adopts the bilayer structure on hydration.<sup>18,19</sup> Cryo-TEM studies revealed that increasing proportions of ESM result in a progressive transition from the commonly observed<sup>20–22</sup> spherical solid-core structure seen for LNP containing 10 mol % ESM to an elongated structure containing a solid core surrounded by a bilayer for systems con-

taining 40 mol % or higher ESM (Figures 1D–1F). LNP mRNA systems containing 40 mol % ESM showed the most homogeneous structures.

### LNP mRNA systems containing 40 mol % ESM or DSPC exhibit increased mRNA expression *in vitro* compared with LNP mRNA systems with the Onpattro formulation containing 10 mol % helper lipids

As noted, LNP systems containing 40 mol % ESM exhibit homogeneous morphology bounded by a lipid bilayer that could be consistent with extended circulation lifetimes. The next question was whether they could be transfection potent. We first examined transfection potency *in vitro*. The effect of increasing the proportions of ESM and DSPC from 10 mol % (Onpattro formulation) to 40 mol % (ESM or DSPC/MC3/Chol/PEG-lipid 40:33:25.5:1.5 mol/mol) on the cellular uptake and transfection potency of LNP containing luciferase mRNA was examined in HuH7 (human-derived hepatocarcinoma) cells. LNP luc mRNA formulations were prepared using an N/P ratio of 6 (a ratio that is commonly used *in vivo*<sup>23–27</sup>), and contained 0.2 mol % of the fluorescent dye 1,1'-dilinoleyl-3,3,3',3'-tetramethylindocarbocyanine perchlorate (DiI). HuH7 cells were incubated with 0.03–3 µg LNP luc mRNA/mL for 24 h and luciferase expression was quantified by measuring luminescence as detailed in methods.

As shown in Figure 2A, LNPs containing 40 mol % DSPC or ESM were significantly more potent transfection systems *in vitro* than the LNPs containing 10 mol % DSPC or ESM. Incubation (24 h) of HuH7 cells with LNP Luc mRNA formulations (0.3 µg mRNA/mL) containing 40 mol % ESM resulted in a 100-fold increase in luciferase expression compared with the 10 mol % DSPC formulation. At all doses tested for both helper lipids, the luminescence was considerably higher for LNP luc mRNA systems containing 40 mol % helper lipid formulations compared with those containing 10 mol % helper lipid. Although the LNP containing 40 mol % helper lipid exhibited higher (~30%) levels of uptake compared with systems containing 10 mol % helper lipid as assayed by mean fluorescence intensity (MFI) of the incorporated fluorescent dye at 24 h post transfection (Figure 2B), such increases cannot account for the orders of magnitude improvement in transfection potency. These results lead to two conclusions. First, increasing the proportions of helper lipids in LNP mRNA systems to 40 mol % dramatically enhances transfection potency *in vitro* compared with LNP mRNA with the 10% DSPC (Onpattro) lipid composition. Second, LNP mRNA systems containing 40% ESM are significantly more potent transfection agents *in vitro* than LNP systems containing 40 mol % DSPC. Liposomal formulations consisting of ESM and cholesterol can achieve circulation lifetimes approaching those achieved for “stealth” liposomes containing high concentrations of PEG-lipids.<sup>16</sup> Thus, LNP mRNA systems containing 40% ESM have the potential to both enhance transfection potency *in vivo* and prolong circulation lifetimes leading to a wider range of tissues that the LNP mRNA can access and potentially transfect.

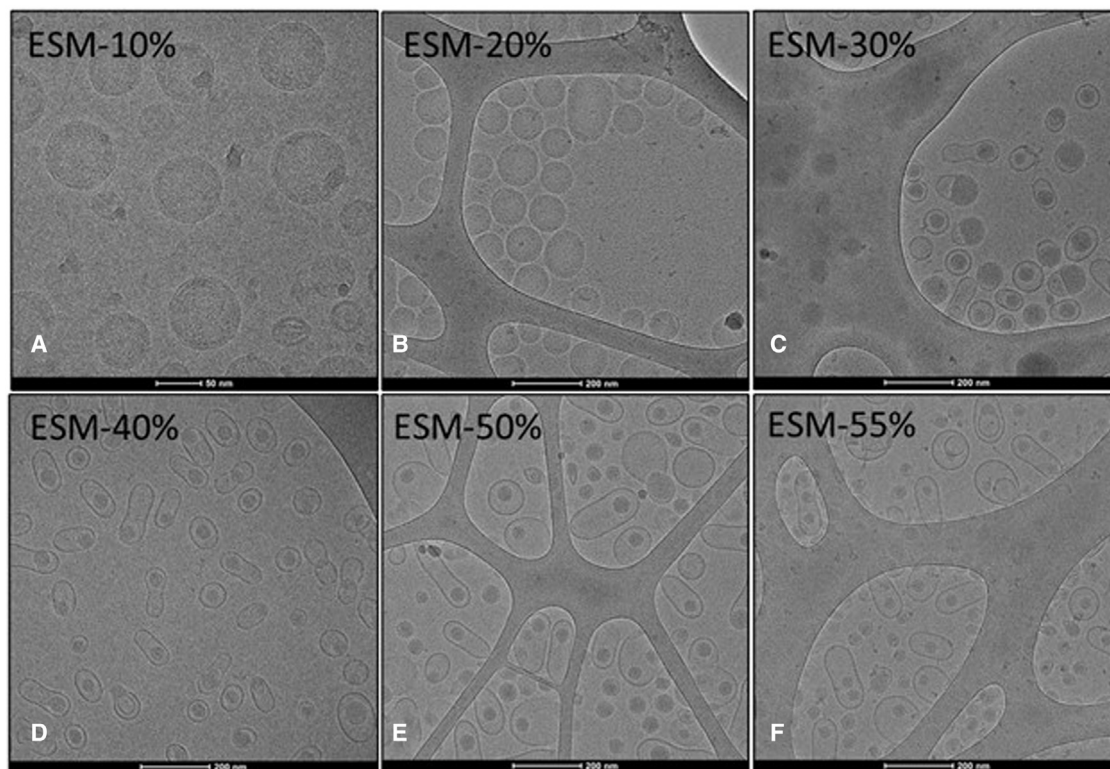


**Figure 1. LNP luc mRNA morphology progress from a solid core structure to a bilayer structure surrounding an aqueous compartment containing a small solid core as the ESM helper lipid content is increased**

LNP luc mRNA systems were formulated at an N/P ratio of 6 as described in methods to contain increasing amounts of the helper lipid egg sphingomyelin (ESM). (A) LNP composition ESM/MC3/Chol/PEG-lipid 10:50:38.5:1.5 mol/mol, (B) LNP composition ESM/MC3/Chol/PEG-lipid 20:44.25:34.25:1.5 mol/mol, (C) LNP composition ESM/MC3/Chol/PEG-lipid 30:38.5:30:1.5 mol/mol, (D) LNP composition ESM/MC3/Chol/PEG-lipid 40:33:25.5:1.5 mol/mol, (E) LNP composition ESM/MC3/Chol/PEG-lipid 50:27.25:21.25:1.5 mol/mol, (F) LNP composition ESM/MC3/Chol/PEG-lipid 55:24.5:19:1.5 mol/mol. For other details see [Table S1](#).

#### **LNP systems containing 40 mol % ESM exhibit improved mRNA stability in the presence of serum**

As noted in [Figure 1](#), LNP mRNA systems containing 40 mol % ESM exhibit a bilayer structure surrounding an aqueous region containing a solid core. Previous work would suggest that the interior solid core contains the neutral form of the ionizable lipid and the mRNA surrounded by a lipid monolayer. If this is the case then it is possible that the mRNA would be better protected from external nucleases than mRNA contained in Onpatro-type systems containing 10 mol % DSPC, which exhibit only an external monolayer.<sup>15</sup> To determine whether this was the case we tested the stability of mRNA coding for GFP (GFP-mRNA) encapsulated in the 40% ESM formulation relative to an Onpatro formulation containing 10% DSPC. We used GFP-mRNA in this and subsequent *in vivo* experiments as a quantitative assessment of GFP expression *in vivo* in individual cells of various tissues can be achieved when GFP fluorescence is measured by flow cytometry.

The mRNA stability data obtained by the Bioanalyser analysis (see methods) are presented in [Figure 3](#). As shown, naked mRNA was immediately degraded in serum, as also demonstrated by flattening

of the mRNA peaks in the electropherogram and the disappearance of related bands in the gel images (see [Figure S2](#)). LNP mRNA encapsulated in LNPs with the Onpatro lipid composition (DSPC/MC3/Chol/PEG-lipid 10:50:38.5:1.5 mol/mol) underwent degradation at a rate of 20% per hour on incubation in 50% fetal bovine serum (FBS). In contrast, the mRNA encapsulated in LNPs containing 40% ESM (ESM/MC3/Chol/PEG-lipid 40:33:25.5:1.5 mol/mol) only exhibited appreciable degradation at the 24 and 48 h time points indicating a degradation rate as low as 5% per hour.

#### **LNP mRNA systems containing 40 mol % ESM exhibit longer circulation lifetimes and increased extrahepatic distribution following i.v. administration compared with LNP mRNA systems with Onpatro lipid compositions**

As noted, LNP with an external lipid bilayer consisting of ESM/Chol should exhibit extended circulation lifetimes as suggested by the stealth characteristics of liposomal systems consisting of ESM/Chol.<sup>16</sup> To determine whether this was the case, we investigated the pharmacokinetic properties of LNP GFP mRNA systems prepared with the Onpatro composition (10 mol % DSPC) or the formulation

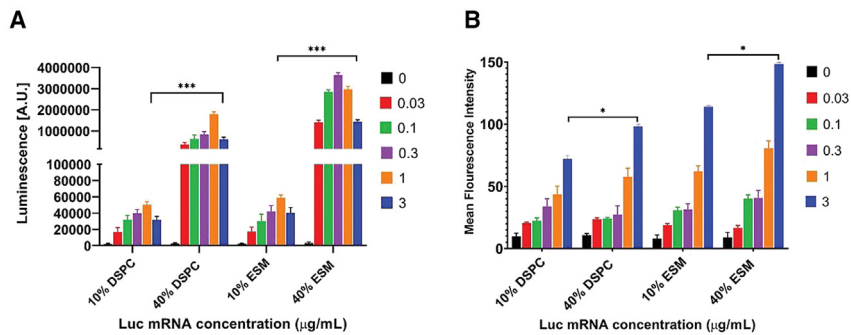


**Figure 2. LNP mRNA system containing high helper lipid contents exhibit dramatically improved transfection potencies compared with Onpatro-type formulations *in vitro***

HuH7 cells were incubated with LNP luc mRNA systems containing DSPC or ESM at 10 or 40 mol % levels over a dose range of 0.03–3 µg mRNA/mL. Luciferase expression (luminescence) was quantified after a 24 h incubation. (A) Luminescence observed for each formulation and dose. Data represent the arithmetic mean  $\pm$  SD of three replicates. (B) Bar graphs depicting the mean fluorescence intensity (MFI) of HuH7 cells indicating the uptake of DiI-labeled LNPs. Data represent the arithmetic mean  $\pm$  SD of three replicates and are normalized for the higher lipid content of 40 mol % systems as described in methods. \* $p < 0.05$ , \*\*\* $p < 0.001$ .

containing 40 mol % ESM and the fluorescent lipid label DiI following i.v. administration. DiI could be used to follow blood clearance.<sup>28</sup> As shown in Figure 4, LNP systems containing 40 mol % ESM exhibited a significantly longer circulation lifetime as indicated by a half-life of 3.7 h for the 40% ESM formulation compared with 15 min for the 10% DSPC formulation. As a result, we refer to the LNP mRNA systems containing 40 mol % ESM as “long-circulating” LNP, or lCLNP.

The biodistribution of LNP GFP mRNA in the heart, lung, liver, spleen, kidney, and bone marrow was also measured following systemic administration of the DiI-labeled LNP GFP mRNA systems. As shown in Figure 5, increased accumulation of LNP with the Onpatro composition (10 mol % DSPC) was observed in the liver compared with LNP containing 40 mol % ESM, whereas the lCLNP containing 40 mol % ESM exhibited greater accumulation in the spleen and bone marrow.

#### LNP mRNA systems containing 40 mol % ESM exhibit improved transfection potency relative to LNP with the Onpatro-type lipid composition in the liver, spleen, and bone marrow

The major objective of this study was to develop transfection-competent lCLNP mRNA systems that could result in greater accumulation of LNP mRNA in extrahepatic tissues such as the bone marrow. Given the apparent tropism of the lCLNPs containing 40 mol % ESM for bone marrow and spleen we examined protein expression in both tissues (as well as liver) for Onpatro LNP GFP mRNA and lCLNP GFP mRNA following systemic administration (3 mg mRNA/kg) in mice. Translation of GFP in liver, spleen, and bone marrow was investigated at a cellular level using flow cytometry, the uptake in hepatocytes, splenocytes, and bone marrow cells was assessed using the fluorescence arising from trace levels of DiI. The details regarding gating strategies can be found in the methods.

Considerable LNP accumulation was observed in hepatocytes for both Onpatro and lCLNP formulations at 4 and 24 h post injection. At 24 h, LNP accumulation was detected in 60% and 70% of hepatocytes for the 10% and 40% ESM formulations, respectively (Fig-

ure 6A). For both formulations the percentage of DiI-positive cells increased significantly from 4 to 24 h (Figure 6A). Remarkably, the proportion of hepatocytes expressing GFP at both 4 and 24 hours post infection was significantly higher for LNP mRNA containing 40% ESM compared with the 10% ESM formulation (Figure 6B) or the classic Onpatro formulation containing 10 mol % DSPC (see Figures S1A and S1B).

In the case of the spleen, LNP GFP mRNA systems containing 40 mol % ESM exhibited preferential distribution to the spleen relative to LNP GFP mRNA containing 10% ESM at both 4 and 24 h post injection (Figure 7A). The proportion of splenocytes expressing GFP was similar for LNP containing both 10 and 40 mol % ESM. However, the LNP mRNA containing 40% ESM exhibited enhanced GFP translation in splenocytes relative to systems containing 10% ESM at both 4 and 24 h post injection (Figure 7B) as well as the classic Onpatro formulation containing 10 mol % DSPC (see Figures S1A and S1B).

As shown in Figure 8B, i.v. administration of LNP GFP mRNA formulations containing 40% ESM led to significantly greater expression in bone marrow cells compared with the 10% ESM formulations at 24 h post injection. At 4 h similar levels of transfection were observed for LNPs containing 10 mol % DSPC or 10 mol % ESM vs. 40 mol % ESM, with the latter showing significantly higher levels of GFP expression (Figure S1). In short, the results presented in this section show that i.v. administration of lCLNP GFP mRNA formulations containing 40 mol % GFP give rise to similar or improved protein expression in liver, spleen, and bone marrow compared with systems containing 10 mol % ESM or classic Onpatro-type systems containing 10 mol % DSPC.

Finally, toxicity studies demonstrated that the newly developed formulations as well as the Onpatro-based LNP mRNAs were well tolerated and did not cause any adverse effect, as assessed by clinical observations, weight measurements, and the chemistry and cytokine panel. During the follow up, a very slight weight loss was observed 24 h post injection, which was regained after 48 h (Figure S4A). Liver function remained largely intact despite a significant accumulation of

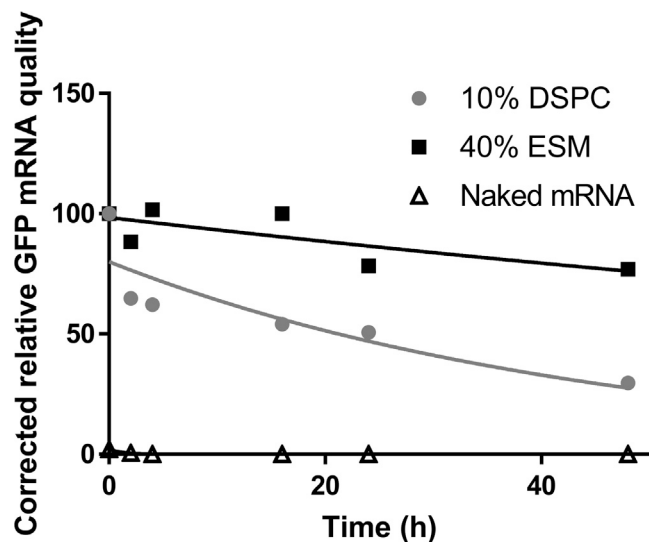


**Figure 3. mRNA encapsulated in LNP containing high levels of helper lipid exhibits improved stability properties when incubated with serum compared with free mRNA or mRNA encapsulated in Onpattro-type LNP formulations**

LNP GFP mRNA systems containing 10% DSPC (DSPC/MC3/Chol/PEG-lipid 10:50:38.5:1.5 mol/mol) or 40% ESM (ESM/MC3/Chol/PEG-lipid 40:33:25.5:1.5 mol/mol) were prepared as described in methods (N/P = 6) and were incubated in 50% FBS at 37°C for 48 h mRNA stability was assessed using an Agilent 2100 Bioanalyzer (see methods). Data are representative of two separate experiments.

LNP mRNAs. The chemistry panel revealed only a slight elevation of two liver enzymes 24 h post injection, which returned to normal 48 h later (Figure S4B). Also, no alteration of blood chemistry was noted, demonstrating an intact kidney function and electrolyte balance. Finally, from the cytokine panel, only IL-1 $\alpha$  and IL-6 were slightly elevated at the 48 h time point, overall demonstrating that the LNP mRNAs did not exhibit any significant immunogenicity with no serious adverse effect on animals (Figures S4C and S4D).

## DISCUSSION

The results presented here demonstrate that, by adjusting the amount and type of helper lipid, LNP mRNA systems can be achieved that result in enhanced expression at 4 and 24 h post administration in target tissues such as liver, spleen, and bone marrow compared with classical Onpattro formulations that contain 10 mol % DSPC. There are three aspects of these results that warrant further discussion. First, the LNP mRNA systems containing 40 mol % ESM exhibit a unique morphology with an outer monolayer surrounding an inner solid core as visualized by cryo-TEM studies, requiring discussion of how such structures may be generated and the benefits in terms of circulation lifetimes and mRNA stability. Second, the results presented here demonstrate that LNP mRNA systems containing 40 mol % of helper lipids such as DSPC or ESM can be highly effective transfection vehicles *in vitro* and that systems containing 40 mol % ESM are also highly effective *in vivo*. This contrasts with previous studies that suggest 10 mol % DSPC results in optimized gene silencing *in vivo* for

LNP siRNA systems. Finally, the potential utility of these systems for transfection of hepatic and extrahepatic tissues is of interest. We discuss these topics in turn.

LNP mRNA systems containing 40 mol % helper lipid exhibit a novel morphology with a bilayer surrounding an inner solid core. Related structures observed for LNP siRNA systems containing high levels of helper lipid have been interpreted as a core of siRNA complexed with ionizable lipid, as well as ionizable lipid in the neutral (oil) form, surrounded by a monolayer of helper lipid/cholesterol suspended in an aqueous environment, which is in turn surrounded by a bilayer consisting of helper lipid/cholesterol.<sup>15</sup> A similar interpretation can be made for the mRNA containing systems, where the interior solid core contains the mRNA. The mechanism whereby these LNP mRNA systems are formed using the rapid mixing/ethanol dilution process can be suggested to begin with formation of a hydrophobic mRNA-ionizable lipid core at pH 4 surrounded by a monolayer of helper lipid/cholesterol that fuses with smaller empty vesicles as the pH is raised due to the conversion of the ionizable cationic lipid to the neutral form.<sup>15,29</sup> As the larger LNP systems form, the ratio of surface lipid (e.g., ESM/Chol) to core lipid (the neutral form of the ionizable cationic lipid) increases and eventually exceeds the amount needed to form the external monolayer. At this point the bilayer lipid progressively forms blebs. At high enough helper lipid contents, the exterior bilayer-preferring helper lipid can form a complete bilayer around the interior hydrophobic core.

The observation that LNP mRNA systems containing high (40 mol %) levels of “helper” lipids such as ESM exhibit comparable or superior levels of protein expression as compared with LNP mRNA with the Onpattro composition *in vitro* and *in vivo* has not been reported previously. This is perhaps surprising considering the large amount of work performed to optimize the transfection properties of LNP formulations of siRNA and mRNA. However, an overwhelming proportion of this work has focused on optimizing the cationic lipid component and has largely concerned studies on *in vivo* properties of these LNP systems.<sup>30</sup>

The enhanced *in vitro* transfection potency of LNP mRNA systems containing ESM, as opposed to DSPC, could be related to enhanced cellular uptake as the ESM formulations exhibited improved uptake into the HuH7 cells compared with systems containing DSPC (Figure 2B). However, the mechanism whereby LNP mRNA systems containing 40 mol % DSPC or ESM elicit dramatically enhanced protein expression *in vitro* compared with systems containing 10 mol % DSPC or ESM (Figure 2A) cannot be ascribed to increased uptake and is not currently understood. In particular, the enhanced transfection potency of systems containing high helper levels would appear to disagree with the proposed mechanism of action for endosomal escape whereby optimized LNP mRNA systems destabilize bilayer structure in the endosome on protonation of the ionizable cationic lipid component due to formation of non-bilayer structures.<sup>31</sup> This is because helper lipids such as DSPC and ESM prefer bilayer structure and would be expected to mitigate against

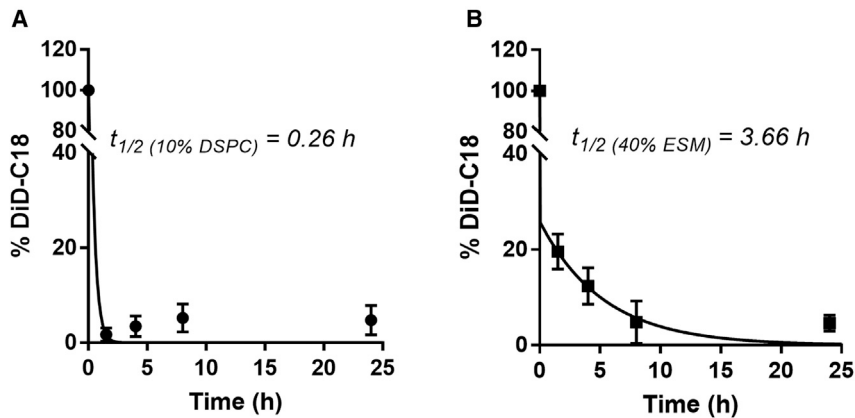


**Figure 4. LNP mRNA systems containing 40 mol % ESM exhibit longer circulation lifetimes following i.v. administration than Onpattro-type formulations**

DiD-labeled LNP GFP mRNA were administered at a dose of 1.5 mg mRNA/kg and blood was collected via the saphenous vein at 0, 1.5, 4, 8, and 24 h. The circulating LNP levels were determined by measuring the DiD fluorescent intensity from collected blood. Each data point represents the arithmetic mean  $\pm$  SD of data collected from five mice. (A) LNP GFP mRNA systems with the Onpattro lipid composition (DSPC/MC3/Chol/PEG-lipid 10:50:38.5:1). (B) LNP GFP mRNA systems containing 40 mol % ESM (ESMMC3/Chol/PEG-lipid 40:33:25.5:1.5).

formation of non-bilayer structures that destabilize the endosomal membrane.<sup>32</sup> It is possible that changes in the structure of these LNPs increases the availability of the solid core as the pH is lowered in the endosome; these and other possibilities are under investigation.

The fact that the 40 mol % ESM systems are more transfection potent *in vivo* in the liver following i.v. administration than classical Onpattro systems containing 10 mol % ESM or DSPC is surprising as extensive efforts have been made to achieve optimized systems for liver (hepatocyte) transfection following i.v. administration. As noted, almost all these optimization efforts for mRNA have focused on LNP with the Onpattro-type lipid composition and have been aimed at developing improved ionizable cationic lipids.<sup>1,30</sup> Work that has been reported for systems containing helper lipid concentrations as high as 40 mol % has focused mainly on the tropism exhibited by LNPs with different helper lipid species and direct comparisons with the properties of LNP mRNA systems with Onpattro lipid compositions are lacking.<sup>33,34</sup> It is perhaps not surprising that LNP lipid compositions optimized for siRNA delivery to the liver are not optimal for delivery of mRNA. As noted, reasons for the enhanced transfection properties of LNP mRNA systems containing 40 mol % ESM could include the improved stability of the encapsulated mRNA as well as the enhanced transfection potency following uptake into cells as indicated by the *in vitro* results presented here.

There are many other factors that could also play a role in increasing transfection potency for the high-ESM LNP system. For example, the protein corona adsorbed by the LNPs in the presence of serum proteins can dramatically affect cell tropism.<sup>35</sup> In addition, it should be noted that a dose based on mg mRNA/kg body weight of the LNP mRNA systems containing high levels of helper lipids such as ESM results in more LNPs per dose with a lower number of copies of mRNA per LNP. For instance, for LNP mRNA systems prepared at an N/P value of 6 with a diameter of 50 nm it can be calculated that a dose of LNP with the ESM/MC3/Chol/PEG-lipid (40:33:25.5:1.5 mol/mol) lipid composition contains approximately 1.7 times as many LNPs compared with an equivalent dose of LNP

with the Onpattro lipid composition. Furthermore, if it is assumed that all of the LNPs contain mRNA it can be calculated that the average number of mRNA per LNP decreases from  $\sim$ 2.1 copies per LNP for the Onpattro composition to  $\sim$ 1.3 for the LNP containing 40 mol % ESM. However, as noted by Li et al., cryo-TEM and other common nanoparticle characterization methods such as small-angle neutron scattering, NMR, and nanoparticle tracking analysis, could not effectively resolve these payload characteristics at the single-nanoparticle level, primarily due to difficulty in distinguishing empty LNPs from those with a payload, and in quantifying mRNA molecules in mRNA-loaded LNPs.<sup>36</sup> In addition, the amount of ionizable lipid per LNP is reduced by the same proportion, which could be rectified by somewhat higher N/P values. All these factors could play a role in affecting transfection properties. For instance, it is well known that higher lipid doses lead to longer circulation lifetimes for liposomal LNP systems,<sup>37</sup> consistent with the longer circulation lifetimes of the LNP containing 40 mol % ESM.

The ability of the 40 mol % ESM systems to elicit improved protein expression in the spleen and bone marrow is likely related to the enhanced distribution to these tissues due to the longer circulation lifetimes as well as the enhanced transfection potency of the LNPs containing 40 mol % ESM. It is interesting to note that the circulation lifetimes achieved (3.7 h) are relatively modest; circulation lifetimes in excess of 10 h can be achieved for DSPC/Chol systems at high (100 mg lipid/kg) dose levels.<sup>37</sup> The lipid dose level corresponding to a dose of 1.5 mg mRNA/kg for an N/P value of 6 is 66 mg lipids/kg. Liposomes consisting of bilayer lipid mixtures such as DSPC/Chol are very well tolerated, doses as high as 1 g lipids/kg have been administered with no observable adverse effects.<sup>37</sup> Higher lipid doses would be expected to lead to longer circulation lifetimes and possibly improved extrahepatic transfection properties.

In summary, the results of this study clearly indicate that SCL LNP mRNA systems containing high levels of helper lipids such as ESM can exhibit improved transfection properties *in vitro* compared with LNPs with the standard Onpattro formulation and that such systems can also provide enhanced transfection levels *in vivo* for

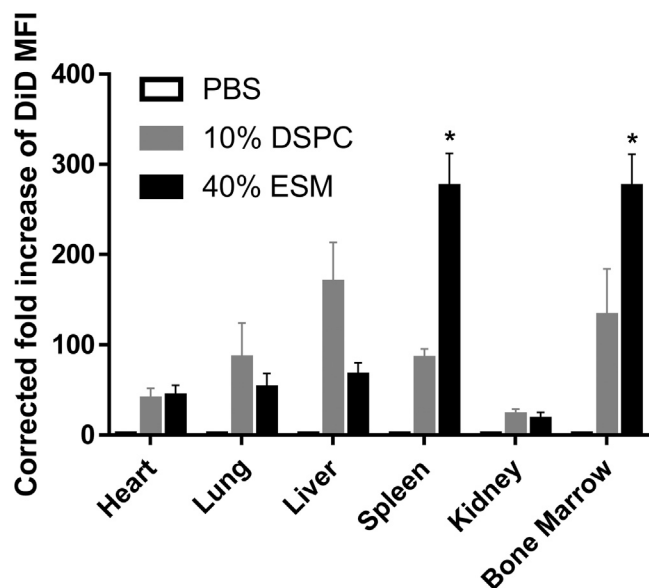


**Figure 5. LNP GFP mRNA systems containing 40 mol % ESM exhibit enhanced accumulation in spleen and bone marrow 48 h post injection compared with LNP GFP mRNA systems with Onpatro (10 mol % helper lipid) lipid compositions**

DiD-labeled LNP GFP mRNA were administered i.v. at a dose of 1.5 mg mRNA/kg. LNP GFP mRNA systems with the Onpatro lipid composition contained DSPC/MC3/Chol/PEG-lipid 10:50:38.5:1. LNP GFP mRNA systems containing 40 mol % ESM had the lipid composition ESM/MC3/Chol/PEG-lipid 40:33:25.5:1.5. Organs were isolated 48 h post administration and DiD fluorescence was determined in cell isolates using flow cytometry. The MFI was calculated from the FACS contour plots (see methods) and normalized to PBS-treated values. Bar graphs depict mean fold increase of DiD in indicated tissues. Each data point represents arithmetic mean  $\pm$  SD of five mice. \* $p < 0.05$ .

hepatic and non-hepatic tissues without any adverse effects. These systems exhibit novel structures characterized by an external lipid bilayer surrounding a solid core suspended in an aqueous interior. The improved transfection properties are due, at least in part, to processes that occur subsequent to cellular uptake and could also reflect improved stability of the mRNA cargo in the LNP interior due to the protective lipid bilayer. The improved circulation lifetimes are consistent with the presence of an exterior lipid bilayer and it is likely that longer circulation lipids and improved bio-distribution and transfection can be achieved for higher lipid doses. It is concluded that these LNP mRNA systems containing high levels of the helper lipid ESM provide a promising approach for achieving improved hepatic and extrahepatic transfection following i.v. administration.

## MATERIALS AND METHODS

### Materials

The lipids DSPC and ESM were purchased from Avanti Polar Lipids (Alabaster, AL). The ionizable cationic lipid heptatriacont-6,9,28,31-tetraen-19-yl 4-(dimethylamino)butanoate (DLin-MC3-DMA; MC3) was synthesized by Biofine International (Vancouver,

BC, Canada). Cholesterol, sodium acetate, Dulbecco's phosphate-buffered saline (PBS), FBS, and Triton X-100 were purchased from Sigma-Aldrich (St. Louis, MO). (R)-2,3-bis(octadecyloxy)propyl-1-(methoxy polyethylene glycol 2000) carbamate (PEG-DMG) was provided by Alnylam Pharmaceuticals. Lipid tracers 1,1'-dioctadecyl-3,3,3',3'-tetramethylindocarbocyanine perchlorate (DiI-C18) and 1,1'-dioctadecyl-3,3,3',3'-tetramethylindocarbocyanine, 4-chlorobenzenesulfonate Salt (DiD-C18) were purchased from Invitrogen (Burlington, ON). Dulbecco's modified Eagle's medium (DMEM) was purchased from Thermo Fischer Scientific. Luciferase mRNA was provided by Dr. Drew Weismann's lab (University of Pennsylvania). CleanCap EGFP mRNA (5moU) was purchased from TriLink Biotechnologies (San Diego, CA).

### Methods

#### LNP mRNA preparation using T-tube mixing

Ionizable amino-lipid (DLin-MC3-DMA), helper lipid (DSPC or ESM), cholesterol, and PEG-DMG were dissolved in ethanol at varying mole ratios. The lipids in ethanol and mRNA prepared in 25 mM acetate buffer (pH 4.0) were combined using the T-tube formulation method at total flow rate of 20 mL/min and flow rate ratio of 3:1 aqueous/organic phases (v/v). Following formulation, particles were dialyzed against Dulbecco's PBS (pH 7.4) using 12–14 kDa regenerated cellulose membranes (Spectrum Labs, Rancho Dominguez, CA) overnight to remove residual EtOH.

#### Analysis of LNP size and morphology

LNP size and morphology were determined using cryo-TEM as described previously.<sup>38,39</sup> LNP size (number mean) and PDIs were further confirmed by dynamic light scattering using the Malvern Zetasizer NanoZS (Worcestershire, UK). Total lipid was determined by measuring the cholesterol content using the Cholesterol E assay (Wako Chemicals, Richmond, VA) at an absorbance of 260 nm.

#### Analysis of mRNA encapsulation efficiency

mRNA encapsulation efficiency was determined using the Quant-iT Ribogreen RNA assay (Life Technologies, Burlington, ON). In brief, LNP mRNA was incubated at 37°C for 10 min in the presence or absence of 1% Triton X-100 (Sigma-Aldrich, St. Louis, MO) followed by the addition of the Ribogreen reagent. The fluorescence intensity (Ex/Em = 480/520 nm) was determined and samples treated with Triton X-100 represent total mRNA while untreated samples represent unencapsulated mRNA.

#### Cryo-TEM

LNPs loaded with mRNA were concentrated (Amicon Ultra-15 Centrifuge Filter Units, Millipore, Billerica, MA) to a total lipid concentration of  $\sim$ 25 mg/mL prior to analysis. Formulations were deposited onto glow-discharged copper grids and vitrified using an FEI Mark IV Vitrobot (FEI, Hillsboro, OR). Cryo-TEM imaging was performed using a 200 kV Glacios microscope equipped with a Falcon III camera at the UBC High Resolution Macromolecular Cryo-Electron Microscopy facility (Vancouver, BC, Canada).

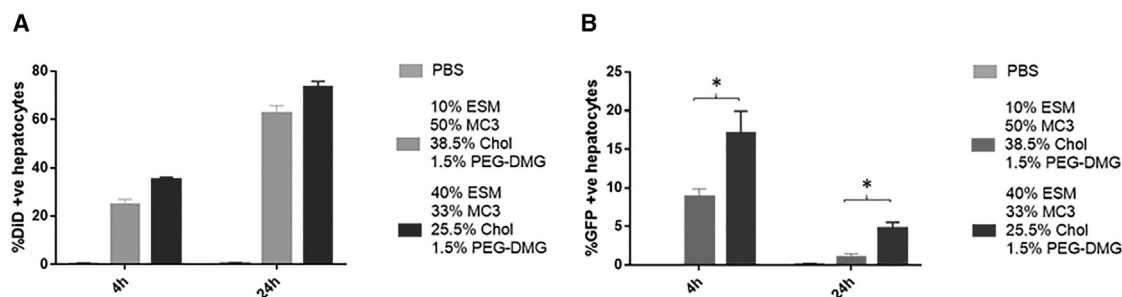


**Figure 6. LNP GFP mRNA systems containing 40 mol % ESM exhibit superior protein expression in liver (C57B16 mice) at 4 and 24 h post injection compared with systems containing 10 mol % ESM**

Flow cytometry results showing LNP uptake and GFP expression in hepatocytes. For original flow data see Figure S3A. (A) Bar graphs represent the arithmetic mean  $\pm$  SD of the percentage of DiD+ cells and (B) the arithmetic mean  $\pm$  SD of the percentage of cells co-expressing DiD and GFP. \* $p < 0.05$ . The data represent three measurements of duplicate mice in three different experiments.

#### **In vitro protein expression assay for LNP mRNA**

Luciferase protein expression was performed using HuH7 cell hepatocyte-derived carcinoma cell line. Growth medium was composed of DMEM with FBS (10%). Cells were plated in 96-well cell culture-treated plates (Falcon/Corning, Corning, NY) at a density of 12,500 cells/well approximately 24 h before treatment. LNP RNA in PBS were diluted as necessary with PBS and added to the appropriate volume of medium to obtain final treatment concentrations of 0, 0.03, 0.1, 0.3, 1, and 3  $\mu\text{g}/\text{mL}$  mRNA concentrations. Treated cells analyzed for luciferase expression after 24 h. Cells were lysed using the Glo lysis buffer and treated with the luciferase reagent (both from Promega, Madison, WI) followed by a readout using a luminometer. To analyze cellular uptake, 0.2 mol % DiI was included in the lipid mix during the formulation process. Following incubation with the formulations under investigation, the plate was washed, fixed and inserted into the Cellomics tray to assess the DiI signal. Uptake analysis based on MFI was determined using Cellomics (Thermo Fisher Scientific, Pittsburgh, PA).

#### **LNP mRNA stability assay**

The stability of LNP mRNA formulations circulating in the biological systems is a determining factor for their activity. Therefore, the ability of mRNA coding for GFP in LNPs comprising 40 mol % helper lipid to endure degradation *in vitro* when incubated in serum, relative to a formulation containing 10 mol % helper lipid content, was investigated. For this, GFP mRNA encapsulated in 10% DSPC (MC3-50%) and 40% ESM (MC3-33%) were incubated in 50% FBS for 0, 2, 4, 8, 16, and 24 h at 5  $\mu\text{M}$  dose. Naked GFP mRNA and MC3-33% were also incubated in 50% FBS and PBS and acted as negative and positive controls, respectively. At the indicated time points, mRNA was extracted from the LNP mRNA formulations following the manufacturer's instructions using a PureLink RNA Mini Kit (Thermo Fisher Scientific). Extracted RNAs were also loaded into an RNA Chip kit and mRNA integrity was determined by automated electrophoresis using an Agilent 2100 Bioanalyzer. Electropherograms of the mRNA samples were generated and Agilent 2100 Expert Software (Agilent Technologies) was used to determine mRNA qual-

ity in the formulation following incubation in PBS or serum. Following the manufacturer's instructions, mRNA integrity was determined using the individual electropherograms generated by drawing appropriate regions including the peak corresponding to the intact mRNA consistent with the 996 nucleotide GFP mRNA size and the region indicating degradation of mRNA. A ratio between the intact and the degraded mRNA was generated and expressed as percent corrected area, a function that factorizes the speed of mRNA migration. The ratio of corrected area at 0 time point whereby the mRNA was assumed intact, was considered 100%, and any change toward degradation was calculated relative to this value.

#### **Pharmacokinetic and biodistribution analysis**

For the evaluation of the circulation lifetime of the encapsulated mRNA in LNP in blood, fluorescently labeled LNPs were used.<sup>28</sup> In brief, mice, five per group, were administered systemically with 1.5 mg/kg mRNA of 10% DSPC and 40% ESM LNP mRNA labeled with DiD-C18 or PBS control. Prior to and following systemic administration, 30  $\mu\text{L}$  of blood was collected from the saphenous vein at the indicated times, and plasma were separated through centrifugation at  $10,000 \times g$  for 5 min. Next, 10  $\mu\text{L}$  plasma serum was diluted to 1% Triton X- at 1:1,000 dilution (100  $\mu\text{L}$ ) and fluorescence was measured at Ex/Em 644/663 nm using a Spark Multimode Microplate reader. The percent of DiD-C18 in the blood was determined from a standard curve of DiD-C18 in mouse serum. To investigate the accumulation of DiD-labeled LNP mRNAs in main organs, heart, lungs, liver, spleen, kidney, and femurs were harvested and kept in complete RPMI medium. Next, they were minced in small pieces, passed through a 42  $\mu\text{m}$  Falcon cell strainer and incubated in RPMI medium containing 0.5 mg/mL collagenase IV (Worthington) for 20 min at 37°C. Bone marrow was also collected from the femurs, resuspended in completed RPMI medium, and cultured for 20 min. Next, aliquots of cell suspension from the indicated organs were collected, washed with FACS staining buffer (2% FBS, 1 mM ethylenediaminetetraacetic acid [EDTA], and 0.1% sodium azide), and analyzed using an LSRII flow cytometer (BD Biosciences) and FACSDiva software as described. DiD expression in organs was measured to determine

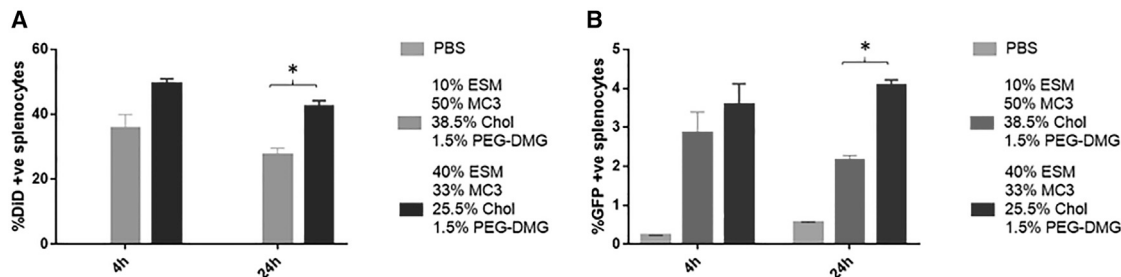


**Figure 7. LNP GFP mRNA systems containing 40 mol % ESM exhibit superior protein expression in spleen (C57B16 mice) at 24 h post injection compared with systems containing 10 mol % ESM**

Flow cytometry results showing LNP uptake and GFP expression in splenocytes. For original flow data see [Figure S3B](#). (A) Bar graphs represent the arithmetic mean  $\pm$  SD of the percentage of DiD+ cells and (B) the arithmetic mean  $\pm$  SD of the percentage of cells co-expressing DiD and GFP. \* $p < 0.05$ . The data represent three measurements of duplicate mice in three different experiments.

LNP mRNA accumulation in targeted organs using the FlowJo software. Assuming that the fluorescence signal is proportional to the lipid content, a normalization factor was calculated by dividing the total lipid of the formulations under investigation (20.6 mg/mL for the Onpatro-based formulation/25.5 mg/mL for 40% DSPC or ESM formulation) equaling 0.81. DiD fluorescence intensity was then corrected by multiplying all MFI values of 10% DSPC and 40% ESM, respectively, by the normalization factor. To calculate the MFI fold increase relative to PBS, the MFI values were divided by the MFI obtained following PBS treatment.

**In vivo analysis of GFP expression**

All mouse protocols were approved by the Canadian Animal Care Committee and conducted in accordance with relevant guidelines and regulations. Mice were maintained on a regular 12 h light/12 h dark cycle in a specific pathogen-free animal facility at UBC. C57Bl6 male mice aged between 8 and 10 weeks were used throughout. These mice were divided into groups of two and received i.v. injection of GFP mRNA-delivered LNPs based on Onpatro, 40 mol % ESM (approach A), or PBS as a negative control. For biodistribution studies, LNPs entrapping GFP mRNA were labeled with 0.2 mol % DiD as fluorescent lipid marker. Injections

were performed at 3 mg/kg mRNA dose and mice were sacrificed at 4 and 24 h post injection. Mice were first anesthetized using a high dose of isoflurane followed by CO<sub>2</sub>. Transcardiac perfusion was performed as follows: once the animals were unresponsive, a 5 cm medial incision was made through the abdominal wall, exposing the liver and heart. While the heart was still beating, a butterfly needle connected to a 30 mL syringe loaded with pre-warmed Hank's balanced salt solution (HBSS) (Gibco) was inserted into the left ventricle. Next, the liver was perfused with perfusion medium (HBSS supplemented with 0.5 mM EDTA, 10 mM glucose, and 10 mM HEPES) at a rate of 3 mL/min for 10 min. Once liver swelling was observed, a cut was performed on the right atrium and perfusion was switched to digestion medium (DMEM, Gibco) supplemented with 10% FBS (Gibco), 1% penicillin streptomycin (Gibco), and 0.8 mg/mL collagenase type IV (Worthington) at 3 mL/min for another 10 min. At the end of the perfusion of the entire system, as determined by organ blanching, the whole liver and spleen were dissected and transferred to 50 mL Falcon tubes containing 10 mL ice-cold (4°C) perfusion medium and placed on ice. Next, isolation of hepatocytes was performed following density gradient-based separation. Spleens and femurs were also harvested to isolate splenocytes and bone marrow cells. In brief, the liver

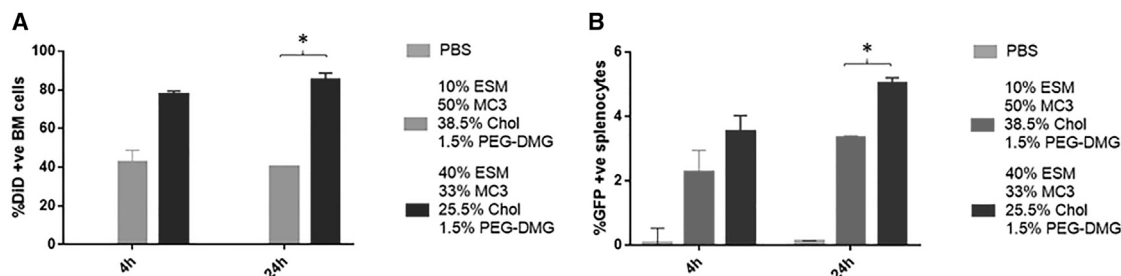


**Figure 8. LNP GFP mRNA systems containing 40 mol % ESM exhibit superior protein expression in bone marrow (C57B16 mice) at 4 and 24 h post injection compared with systems containing 10 mol % ESM**

Flow cytometry results showing LNP uptake and GFP expression in bone marrow cells. For original flow data see [Figure S3C](#). (A) Bar graphs represent the arithmetic mean  $\pm$  SD of the percentage of DiD+ cells and (B) the arithmetic mean  $\pm$  SD of the percentage of cells co-expressing DiD and GFP. \* $p < 0.05$ . The data represent three measurements of duplicate mice in three different experiments.

was transferred to a petri dish containing digestion medium, minced under sterile conditions, and incubated for 20 min at 37°C with occasional shaking of the plate. Cell suspensions were then filtered through a 40 µm mesh cell strainer to eliminate any undigested tissue remnants. Primary hepatocytes were separated from other liver-residing cells by low-speed centrifugation at 500 rpm with no brake. The pellet containing mainly hepatocytes was collected, washed at 5,000 rpm for 5 min, and kept in 4°C. Femurs were centrifuged 10,000 × *g* in a microcentrifuge for 10 s to collect the marrow that was resuspended in ACK lysis buffer for 1 min to deplete the red blood cells followed by washing with ice-cold PBS. Phenotypic detection of hepatocytes was then performed using monoclonal antibodies to assess LNP delivery and mRNA expression. Cellular uptake and GFP expression was also detected in splenocytes and bone marrow cells immediately after isolation. Here, the spleen was dissected and placed into a 40 µm mesh cell and mashed through the cell strainer into the petri dish using the plunger end of the syringe. The suspended cells were transferred to a 15 mL Falcon tube and centrifuged at 1,000 rpm for 5 min. The pellet was resuspended in 1 mL ACK lysis buffer (Invitrogen) to lyse the red blood cells and aliquoted in FACS buffer. Cell aliquots were resuspended in 300 µL FACS staining buffer (FBS 2%, sodium azide 0.1%, and EDTA [1 mM]) followed by staining with fluorescence-tagged antibodies. Prior to staining, cells were first labeled with anti-mouse CD16/CD32 (mouse Fc blocker, Clone 2.4G2) (AntibodyLab, Vancouver, Canada) to reduce background. Hepatocytes were detected following staining with primary mouse antibody detecting ASGR1 (8D7, Novus Biologicals) followed by goat polyclonal secondary antibody to mouse IgG2a labeled to PE-Cy7 (BioLegend). Detection of hepatocytes, splenocytes, and bone marrow cells was acquired using an LSRII flow cytometer and the FACSDiva software and analyzed by FlowJo following acquisition of 1,000,000 events after gating on viable cell populations. LNP mRNA delivery or transfection efficacy were assessed based on the relative MFI of DiD- or GFP-positive cells, respectively, measured on histograms obtained from gated cell populations.

### Toxicity studies

To measure the toxicity of the formulations used *in vivo* in parallel experiments, mice (*n* = 3) for each group were administered *i.v.* with 3 mg/kg LNP mRNA formulated based on Onpatro composition (MC3 50%/ESM 10%/Chol 38.5%/PEG 1.5%), the new composition (MC3 33%/ESM 40%/Chol 25.5%/PEG 1.5%) and saline control. At the 24 h time point post *i.v.* administration, 100 µL of blood was collected from lateral saphenous vein, and under isoflurane anesthesia, 48 h post LNP mRNA administration 1 mL of blood was withdrawn through cardiac puncture. Blood was transferred to MiniCollect K2EDTA and a VACUETTE Z serum clot activator tube with a gel separator, respectively (Fisher Scientific, Ottawa, ON, Canada), allowed to clot at room temperature for 30 min, and centrifuged at 2,000 rpm for 10 min. Serum was then transferred to Eppendorf tubes and kept at 4°C. Custom clinical chemistry tests and a Mouse Cytokine Multiplex Panel were performed by IDEXX BioAnalytics (Delta, BC, Canada) and IDEXX BioAnalytics

(Columbia, MO). Blood analytes were used to assess biomarkers of liver health, general protein concentration, electrolyte balance, metabolic status, acid-base balance and kidney health. In addition, a panel of 10 cytokines in the serum was also measured to assess the immunogenicity of LNP mRNA formulations.

### Statistical analysis

Statistical analyses were performed using a two-tailed Student's *t* test, where groups were compared as indicated. The type (paired or two-sample equal variance-homoscedastic) was determined based on the variation of the standard deviation of two populations. *p* < 0.05 was accepted as statistically significant (\**p* < 0.05).

### DATA AVAILABILITY STATEMENT

All data generated and analyzed during this study are included in this published article and its [supplemental information files](#).

### SUPPLEMENTAL INFORMATION

Supplemental information can be found online at <https://doi.org/10.1016/j.omtm.2023.06.005>.

### ACKNOWLEDGMENTS

The authors would like to acknowledge support from the Canadian Institutes of Health Research (CIHR) under UOP grant 122069 and the NanoMedicines Innovation Network (NMIN), a Canadian Networks of Centres of Excellence (NCE) in nanomedicine. D.W. is supported by the Swiss National Science Foundation (no. 183923). M.H.Y.C. is supported by NMIN's postdoctoral fellowship in gene therapy.

### AUTHOR CONTRIBUTIONS

N.C., D.W., G.B., M.H.Y.C., and P.R.C. designed the experiments. N.C., G.B., and M.H.Y.C. conducted the experiments. N.C., M.H.Y.C., G.B., and P.C. wrote the paper.

### DECLARATION OF INTERESTS

P.R.C. has financial interests in Acuitas Therapeutics, Mesentech, and NanoVation Therapeutics. D.W. has financial interests in NanoVation Therapeutics.

### REFERENCES

- Kulkarni, J.A., Witzigmann, D., Thomson, S.B., Chen, S., Leavitt, B.R., Cullis, P.R., and van der Meel, R. (2021). The current landscape of nucleic acid therapeutics. *Nat. Nanotechnol.* *16*, 630–643.
- Sahin, U., Karikó, K., and Türeci, Ö. (2014). mRNA-based therapeutics—developing a new class of drugs. *Nat. Rev. Drug Discov.* *13*, 759–780.
- Pardi, N., Hogan, M.J., Porter, F.W., and Weissman, D. (2018). mRNA vaccines - a new era in vaccinology. *Nat. Rev. Drug Discov.* *17*, 261–279.
- Rizvi, F., Everton, E., Smith, A.R., Liu, H., Osota, E., Beattie, M., Tam, Y., Pardi, N., Weissman, D., and Gouon-Evans, V. (2021). Murine liver repair via transient activation of regenerative pathways in hepatocytes using lipid nanoparticle-complexed nucleoside-modified mRNA. *Nat. Commun.* *12*, 613.
- Magadam, A., Kaur, K., and Zangi, L. (2019). mRNA-Based Protein Replacement Therapy for the Heart. *Mol. Ther.* *27*, 785–793.

6. Adams, D., Gonzalez-Duarte, A., O’Riordan, W.D., Yang, C.C., Ueda, M., Kristen, A.V., Tournev, I., Schmidt, H.H., Coelho, T., Berk, J.L., et al. (2018). Patisiran, an RNAi Therapeutic, for Hereditary Transthyretin Amyloidosis. *N. Engl. J. Med.* *379*, 11–21.
7. Allen, T.M. (1994). Long-circulating (sterically stabilized) liposomes for targeted drug delivery. *Trends Pharmacol. Sci.* *15*, 215–220.
8. Quick, J., Santos, N.D., Cheng, M.H.Y., Chander, N., Brimacombe, C.A., Kulkarni, J., van der Meel, R., Tam, Y.Y.C., Witzigmann, D., and Cullis, P.R. (2022). Lipid nanoparticles to silence androgen receptor variants for prostate cancer therapy. *J. Contr. Release* *349*, 174–183.
9. Mui, B.L., Tam, Y.K., Jayaraman, M., Ansell, S.M., Du, X., Tam, Y.Y.C., Lin, P.J., Chen, S., Narayanannair, J.K., Rajeev, K.G., et al. (2013). Influence of Polyethylene Glycol Lipid Desorption Rates on Pharmacokinetics and Pharmacodynamics of siRNA Lipid Nanoparticles. *Mol. Ther. Nucleic Acids* *2*, e139.
10. Cullis, P.R., and Hope, M.J. (2017). Lipid Nanoparticle Systems for Enabling Gene Therapies. *Mol. Ther.* *25*, 1467–1475.
11. Cheng, Q., Wei, T., Farbiak, L., Johnson, L.T., Dilliard, S.A., and Siegwart, D.J. (2020). Selective organ targeting (SORT) nanoparticles for tissue-specific mRNA delivery and CRISPR-Cas gene editing. *Nat. Nanotechnol.* *15*, 313–320.
12. Audouy, S.A.L., de Leij, L.F.M.H., Hoekstra, D., and Molema, G. (2002). In vivo characteristics of cationic liposomes as delivery vectors for gene therapy. *Pharm. Res. (N. Y.)* *19*, 1599–1605.
13. Kedmi, R., Ben-Arie, N., and Peer, D. (2010). The systemic toxicity of positively charged lipid nanoparticles and the role of Toll-like receptor 4 in immune activation. *Biomaterials* *31*, 6867–6875.
14. Zhigaltsev, I.V., and Cullis, P.R. (2023). Morphological behavior of liposomes and lipid nanoparticles. *Langmuir* *39*, 3185–3193.
15. Kulkarni, J.A., Witzigmann, D., Leung, J., Tam, Y.Y.C., and Cullis, P.R. (2019). On the role of helper lipids in lipid nanoparticle formulations of siRNA. *Nanoscale* *11*, 21733–21739.
16. Webb, M.S., Harasym, T.O., Masin, D., Bally, M.B., and Mayer, L.D. (1995). Sphingomyelin-cholesterol liposomes significantly enhance the pharmacokinetic and therapeutic properties of vincristine in murine and human tumour models. *Br. J. Cancer* *72*, 896–904.
17. Mayer, L.D., Tai, L.C., Ko, D.S., Masin, D., Ginsberg, R.S., Cullis, P.R., and Bally, M.B. (1989). Influence of vesicle size, lipid composition, and drug-to-lipid ratio on the biological activity of liposomal doxorubicin in mice. *Cancer Res.* *49*, 5922–5930.
18. Cullis, P.R., and Hope, M.J. (1980). The bilayer stabilizing role of sphingomyelin in the presence of cholesterol: a <sup>31</sup>P NMR study. *Biochim. Biophys. Acta* *597*, 533–542.
19. Chiu, S.W., Vasudevan, S., Jakobsson, E., Mashl, R.J., and Scott, H.L. (2003). Structure of sphingomyelin bilayers: a simulation study. *Biophys. J.* *85*, 3624–3635.
20. Crawford, R., Dogdas, B., Keough, E., Haas, R.M., Wepukhulu, W., Krotzer, S., Burke, P.A., Sepp-Lorenzino, L., Bagchi, A., and Howell, B.J. (2011). Analysis of lipid nanoparticles by Cryo-EM for characterizing siRNA delivery vehicles. *Int. J. Pharm.* *403*, 237–244.
21. Eygeris, Y., Patel, S., Jozic, A., and Sahay, G. (2020). Deconvoluting Lipid Nanoparticle Structure for Messenger RNA Delivery. *Nano Lett.* *20*, 4543–4549.
22. Leung, A.K.K., Hafez, I.M., Baoukina, S., Belliveau, N.M., Zhigaltsev, I.V., Afshinmanesh, E., Tieleman, D.P., Hansen, C.L., Hope, M.J., and Cullis, P.R. (2012). Lipid Nanoparticles Containing siRNA Synthesized by Microfluidic Mixing Exhibit an Electron-Dense Nanostructured Core (vol 116, pg 18440, 2012). *J. Phys. Chem. C* *116*, 22104.
23. Oberli, M.A., Reichmuth, A.M., Dorkin, J.R., Mitchell, M.J., Fenton, O.S., Jaklenec, A., Anderson, D.G., Langer, R., and Blankschtein, D. (2017). Lipid Nanoparticle Assisted mRNA Delivery for Potent Cancer Immunotherapy. *Nano Lett.* *17*, 1326–1335.
24. Buschmann, M.D., Carrasco, M.J., Alishetty, S., Paige, M., Alameh, M.G., and Weissman, D. (2021). Nanomaterial Delivery Systems for mRNA Vaccines. *Vaccines (Basel)* *9*.
25. Hassett, K.J., Benenato, K.E., Jacquinet, E., Lee, A., Woods, A., Yuzhakov, O., Himansu, S., Deterling, J., Geilich, B.M., Ketova, T., et al. (2019). Optimization of Lipid Nanoparticles for Intramuscular Administration of mRNA Vaccines. *Mol. Ther. Nucleic Acids* *15*, 1–11.
26. Pardi, N., Tuyishime, S., Muramatsu, H., Kariko, K., Mui, B.L., Tam, Y.K., Madden, T.D., Hope, M.J., and Weissman, D. (2015). Expression kinetics of nucleoside-modified mRNA delivered in lipid nanoparticles to mice by various routes. *J. Contr. Release* *217*, 345–351.
27. Kauffman, K.J., Dorkin, J.R., Yang, J.H., Heartlein, M.W., DeRosa, F., Mir, F.F., Fenton, O.S., and Anderson, D.G. (2015). Optimization of Lipid Nanoparticle Formulations for mRNA Delivery in Vivo with Fractional Factorial and Definitive Screening Designs. *Nano Lett.* *15*, 7300–7306.
28. Sakurai, Y., Mizumura, W., Murata, M., Hada, T., Yamamoto, S., Ito, K., Iwasaki, K., Katoh, T., Goto, Y., Takagi, A., et al. (2017). Efficient siRNA Delivery by Lipid Nanoparticles Modified with a Nonstandard Macrocyclic Peptide for EpCAM-Targeting. *Mol. Pharm.* *14*, 3290–3298.
29. Kulkarni, J.A., Darjuan, M.M., Mercer, J.E., Chen, S., van der Meel, R., Thewalt, J.L., Tam, Y.Y.C., and Cullis, P.R. (2018). On the Formation and Morphology of Lipid Nanoparticles Containing Ionizable Cationic Lipids and siRNA. *ACS Nano* *12*, 4787–4795.
30. Semple, S.C., Leone, R., Barbosa, C.J., Tam, Y.K., and Lin, P.J.C. (2022). Lipid Nanoparticle Delivery Systems to Enable mRNA-Based Therapeutics. *Pharmaceutics* *14*, 398.
31. Semple, S.C., Akinc, A., Chen, J., Sandhu, A.P., Mui, B.L., Cho, C.K., Sah, D.W.Y., Stebbing, D., Crosley, E.J., Yaworski, E., et al. (2010). Rational design of cationic lipids for siRNA delivery. *Nat. Biotechnol.* *28*, 172–176.
32. Cullis, P.R., and de Kruijff, B. (1979). Lipid polymorphism and the functional roles of lipids in biological membranes. *Biochim. Biophys. Acta* *559*, 399–420.
33. LoPresti, S.T., Arral, M.L., Chaudhary, N., and Whitehead, K.A. (2022). The replacement of helper lipids with charged alternatives in lipid nanoparticles facilitates targeted mRNA delivery to the spleen and lungs. *J. Contr. Release* *345*, 819–831.
34. Cheng, X., and Lee, R.J. (2016). The role of helper lipids in lipid nanoparticles (LNPs) designed for oligonucleotide delivery. *Adv. Drug Deliv. Rev.* *99*, 129–137.
35. Francia, V., Schifferers, R.M., Cullis, P.R., and Witzigmann, D. (2020). The biomolecular corona of lipid nanoparticles for gene therapy. *Bioconjugate Chem.* *31*, 2046–2059.
36. Li, S., Hu, Y., Li, A., Lin, J., Hsieh, K., Schneiderman, Z., Zhang, P., Zhu, Y., Qiu, C., Kokkili, E., et al. (2022). Payload distribution and capacity of mRNA lipid nanoparticles. *Nat. Commun.* *13*, 5561.
37. Oja, C.D., Semple, S.C., Chonn, A., and Cullis, P.R. (1996). Influence of dose on liposome clearance: critical role of blood proteins. *Biochim. Biophys. Acta* *1281*, 31–37.
38. Belliveau, N.M., Huft, J., Lin, P.J., Chen, S., Leung, A.K., Leaver, T.J., Wild, A.W., Lee, J.B., Taylor, R.J., Tam, Y.K., et al. (2012). Microfluidic Synthesis of Highly Potent Limit-size Lipid Nanoparticles for In Vivo Delivery of siRNA. *Mol. Ther. Nucleic Acids* *1*, e37.
39. Leung, A.K.K., Tam, Y.Y.C., Chen, S., Hafez, I.M., and Cullis, P.R. (2015). Microfluidic Mixing: A General Method for Encapsulating Macromolecules in Lipid Nanoparticle Systems. *J. Phys. Chem. B* *119*, 8698–8706.